For the origin of the nucleophilic substitution path, which seems common in trinuclear and higher metal clusters,[13b] we offer the following speculation. As found for organometallic radicals[24] a key requirement for the existence of such a path is a suitable acceptor orbital on the metal. When triangular faces of metal atoms occur, then the lowest lying metal localized acceptor orbital is the σ^* orbital for the cyclopropane-like σ bonding network as found in $Ru_3(CO)_{12}$.[25] This orbital is directed out the edge of the cluster as shown in Figure 10 and may be accessible to attack by a nucleophile. In Table XIV we collect several properties relevant to this discussion. The energy of the lowest acceptor orbital follows the order $Co_4 < Rh_4 < Ir_4$ as inferred from optical spectroscopy, and the electrochemical reduction potential measurements, E_{pc}, support this trend. Electrophilic character at the metal as reflected by the cluster core charge calculated by SCF-Xα-DV theory,[5] $\int \rho$, or by the amount of charge donated to the CO ligands, ν(CO), should increase as $Co_4 < Rh_4 \sim Ir_4$. Metal-carbonyl bond strengths inferred from both length data, M-C^{ap}, or from the trend in rates of dissociative CO loss discussed earlier appear to follow the order Rh < Co < Ir. Steric accessibility for nucleophilic attack should also parallel the metal-metal bond lengths, M^{ap}-M^{bas} Co $\ll$ Ir $\sim$ Rh. Poë and co-workers[3b,12] have emphasized that a weakened metal-metal bond should enhance the susceptibility of clusters to associative attack because metal ligand bonding in the associative transition state will reduce the number of electrons involved in cluster bonding. All these factors, some operating in opposition, probably contribute to determining the observed trend in k_2.

Acknowledgment. This material is based on work supported by the National Science Foundation (Grants CHE-85-04088 and CHE-85-14366). We thank Johnson-Matthey, Inc. for a loan of precious metals. The insightful comments of Professor A. J. Poë are gratefully acknowledged.

Supplementary Material Available: Tables of IR carbonyl stretching frequencies, electronic absorption spectral data, anisotropic temperature factors, bond distances and angles, and hydrogen coordinates (14 pages); listing of structure factors (46 pages). Ordering information is given on any current masthead page.

(24) Trogler, W. C. *Int. J. Chem. Kinet.* **1987**, *19*, 1025.
(25) Delley, B.; Manning, M. C.; Ellis, D. E.; Berkowitz, J.; Trogler, W. C. *Inorg. Chem.* **1982**, *21*, 2247.

Stopped-Flow Kinetic Study of the Reaction of $(P(C_6H_{11})_3)_2W(CO)_3(L)$ (L = H_2, D_2, and N_2) with Pyridine. Kinetic Resolution of Reaction of Dihydride versus Molecular Hydrogen Complexes

Kai Zhang, Alberto A. Gonzalez, and Carl D. Hoff*

Contribution from the Department of Chemistry, University of Miami, Coral Gables, Florida 33124. *Received September 14, 1988*

Abstract: The rates of reaction of $(P(C_6H_{11})_3)_2W(CO)_3(L)$ (L = H_2, D_2, and N_2) with pyridine have been studied by stopped-flow kinetics. The molecular nitrogen system shows simple first-order loss of N_2 with a rate constant of 75 s^{-1} at 25 °C and an activation energy of 17.8 ± 0.7 kcal/mol. The rate of reaction of the intermediate $(P(C_6H_{11})_3)_2W(CO)_3$ with N_2 gas is 5.0 ± 1.0 × 10^5 M^{-1} s^{-1} at 25 °C in toluene solution. Reactions of the hydrogen and deuterium complexes are complicated due to the presence of both molecular hydrogen (deuterium) and dihydride (dideuteride) complexes. These data are resolved and interpreted in terms of a rapid loss of molecular hydrogen (k = 469 s^{-1} for H_2 and 267 s^{-1} for D_2 at 25 °C, $\Delta H^{\ddagger}$ = 16.9 ± 2.2 kcal/mol for H_2 and 16.2 ± 1.1 kcal/mol for D_2). The hydride complex, which is present in ~30%, reacts an order of magnitude slower than the molecular hydrogen complex (k = 37 s^{-1} for H_2 and 33 s^{-1} for D_2 at 25 °C), $\Delta H^{\ddagger}$ = 14.4 ± 0.5 kcal/mol for H_2 and 14.7 ± 0.8 kcal/mol for D_2). The rate of addition of H_2 to $(P(C_6H_{11})_3)_2W(CO)_3$ is calculated to be 2.2 ± 0.3 × 10^6 M^{-1} s^{-1} at 25 °C. These data are combined with earlier thermodynamic measurements to generate a reaction profile for binding and oxidative addition of hydrogen to the complex $(P(C_6H_{11})_3)_2W(CO)_3$.

Oxidative addition of H_2 gas is one of the fundamental steps in a number of catalytic processes. It has only recently been recognized that H_2 can coordinate as a molecule,[1] and that such complexes may be precursors to oxidative addition as depicted generally in eq 1. A number of catalytic studies have measured

$$M + H_2 \rightarrow M-(H_2) \rightarrow \begin{matrix} M-H \\ | \\ H \end{matrix} \quad (1)$$

the rate of uptake of hydrogen gas, but relatively few direct measurements of the rate of reaction with hydrogen have been made. In general, metal fragments that will add H_2 are highly reactive and have only transitory existence. The majority of these systems have been studied by flash photolysis.[2,3] A good example[4-11] of these systems is reaction of $Cr(CO)_6$ as described in reaction 2. The initially formed $Cr(CO)_5$ reacts on the picosecond

$$Cr(CO)_6 \xrightarrow{h\nu} Cr(CO)_5 \xrightarrow{a} Cr(CO)_5(C_6H_{12}) \xrightarrow{b} Cr(CO)_5(H_2) \quad (2)$$

time scale to form $Cr(CO)_5$(cyclohexane). This complex contains

(1) Kubas, G. J. *Acc. Chem. Res.* **1988**, *21*, 120, and references therein.
(2) Poliakoff, M.; Weitz, E. *Adv. Organometal. Chem.* **1986**, *25*, 277.
(3) Weitz, E. *J. phys. Chem.* **1987**, *91*, 3945.
(4) Kelly, J. M.; Bent, D. V.; Hermann, H.; Schulte-Frohlinde, D.; Von Gustorf, K. E. *J. Organometal. Chem.* **1974**, *69*, 259.
(5) Lees, A. J.; Adamson, A. W. *Inorg. Chem.* **1981**, *20*, 4381.
(6) Welch, J. A.; Peters, K. S.; Vaida, V. *J. Phys. Chem.* **1982**, *86*, 1941.
(7) Hermann, H.; Grevels, F.-W.; Henne, A.; Schaffner, K. *J. Phys. Chem.* **1982**, *86*, 5151.
(8) Church, S. P.; Grevels, F.-W.; Hermann, H.; Schaffner, K. *Inorg. Chem.* **1984**, *23*, 3830.
(9) Church, S. P.; Grevels, F.-W.; Hermann, H.; Schaffner, K. *Inorg. Chem.* **1985**, *24*, 418.
(10) Church, S. P.; Grevels, F.-W.; Hermann, H.; Schaffner, K. *J. Chem. Soc., Chem. Commun.* **1985**, 30.
(11) Simon, J. D.; Xiaoliang, X. *J. Phys. Chem.* **1987**, *91*, 5538.

0002-7863/89/1511-3627$01.50/0

a three-center Cr···H–C_6H_{11} "agostic" bond. Measurements using photoacoustic calorimetry indicate the strength of the Cr–cyclohexane bond formed in reaction 2a is on the order of 10 kcal/mol.[12] "Naked" $Cr(CO)_5$, and presumably many other "coordinatively unsaturated" complexes appear to react so fast that it may not be possible to characterize them in normal solvents.[13] It is the reactions of the solvated species that are actually observed. This conclusion, which is natural in aqueous solution, has only recently been appreciated in organometallic chemistry. The presence of these "token ligands" serves to slow down the overall reactions of the relatively "hot" coordinatively unsaturated complexes.

Reactions of complexes such as $Cr(CO)_5$(alkane) are nevertheless very rapid. Formation of $Cr(CO)_5(H_2)$ in reaction 2b has been shown to occur with $t_{1/2} = 36$ μs at room temperature and 1.3 atm H_2.[9] This complex, formulated to be a molecular hydrogen complex based on its infrared spectrum, is unstable and decomposes in a few seconds under these conditions. The rate of reaction of $Cr(CO)_5$(alkane) with H_2 is similar to its rate of reaction with N_2 and CO.

A different type of kinetic behavior was observed in reaction of H_2 with $RhCl(PPh_3)_2$. In this case, reaction with H_2 is much slower than with other ligands. Generated by flash photolysis of $RhCl(CO)(PPh_3)_2$, the intermediate $RhCl(PPh_3)_2$ reacts with H_2 with a second-order rate constant $k_1 = 1 \times 10^5$ M^{-1} s^{-1}.[14]

$$RhCl(CO)(PPh_3)_2 \underset{k_{-1}}{\overset{h\nu}{\rightleftharpoons}} CO + RhCl(PPh_3)_2 + H_2 \xrightarrow{k_1} Rh(Cl)(PPh_3)_2(H)_2 \quad (3)$$

This is in agreement with earlier data obtained from stopped-flow studies by Halpern and Wong.[15] While this reaction is fast, it is still some 700 times slower than the rate of the back reaction with CO.

These differences in reactivity show the complex nature of the simple reaction shown in eq 1. We have recently[16] reported calorimetric data on reaction 4. We now report results of our

$$(P(C_6H_{11})_3)_2W(CO)_3 + L \rightarrow (P(C_6H_{11})_3)_2W(CO)_3(L) \quad (4)$$
$$L = H_2, N_2, NCCH_3, \text{pyridine}, P(OMe)_3, CO$$

investigation of the reaction of the H_2, D_2, and N_2 complexes with pyridine. The combination of kinetic and thermodynamic results is used to generate a complete profile for binding of nitrogen and hydrogen in this system.

Experimental Section

All manipulations involving organometallic complexes were done in a Vacuum/Atmospheres glovebox or by using standard Schlenk tube techniques. The complexes $(P(C_6H_{11})_3)_2W(CO)_3(L)$ were prepared as described in the literature.[1] Toluene was distilled from sodium benzophenone ketyl under an argon atmosphere. Pyridine was refluxed several days over barium oxide and then distilled under an argon atmosphere.

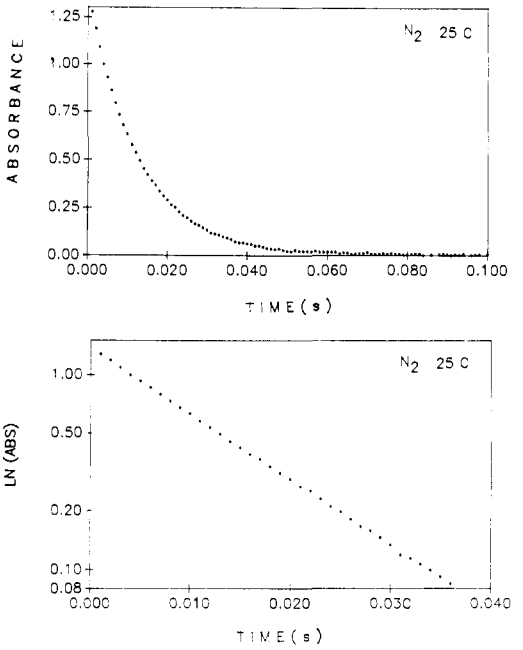

Figure 1. Plots of $A_\infty - A$ on linear (upper) and logarithmic (lower) scales for the reaction W_k–N_2 + py → W_k–py + N_2 at 25 °C.

Table I. Kinetic Data for the Reaction[a] $(P(C_6H_{11})_3)_2W(CO)_3N_2$ + py → $(P(C_6H_{11})_3)_2W(CO)_3$py + N_2

T, °C	$[N_2]/[py]^b$	k_{obsd}, s^{-1}	T, °C	$[N_2]/[py]^b$	k_{obsd}, s^{-1}
35	0	190	25	0.412	58
25	0	75	25	0.824	48
25	0.206	61	15	0	25

[a] Reactions performed in toluene solution under pseudo-first-order conditions as described in text. [b] Reactions performed under N_2 atmosphere; $[N_2]/[py]$ ratios calculations based on known gas solubility data.[11] Values listed as 0 were done under N_2 but at high concentration of pyridine such that $[N_2]/[py] < 0.001$.

Kinetic studies were performed using a Hi-Tech Scientific SF-51 stopped-flow apparatus equipped with a SU-40 spectrophotometer unit. A typical procedure is described below.

The violet complex $(P(C_6H_{11})_3)_2W(CO)_3$ was taken into the glovebox and 0.04 g was loaded into a Schlenk tube under the argon atmosphere in the glovebox. The flask was filled with 50 mL of distilled toluene added via syringe to prepare a solution 9.66×10^{-4} M in the complex. A second flask containing 4 mL of pyridine in 25 mL of toluene, 1.99 M in pyridine, was prepared and both flasks were taken to the Hi-Tech stopped-flow apparatus. A special manifold was used to maintain the hydrogen gas at a pressure of 1.2 atm (CAUTION: several oil bubblers were set up in the line to monitor the flow of hydrogen at all times since it could present an explosion hazard in the area of the stopped-flow unit). The solutions were shaken for ~30 min to ensure that they were saturated with hydrogen gas. The purple solution containing $(P(C_6H_{11})_3)_2W(CO)_3$ turned yellow, indicating complete conversion to the hydrogen complex. The syringes in the stopped-flow apparatus were filled with the solutions. The syringe containing the pyridine solution was flushed twice with solution, and the syringe containing the hydrogen complex was flushed four or five times before beginning each run. The syringes were allowed to equilibrate at the bath temperature for ~30 min. After firing three "shots" quickly without recording the spectrum, a fourth run was recorded. The reaction was monitored by following the buildup of the product $(P(C_6H_{11})_3)_2W(CO)_3$(py) at 545.5 nM. An average of six to eight runs was taken at each temperature and pyridine concentration. The concentration of H_2 was calculated by using known solubility data[21] and assuming Henry's law was applicable. Qualitative experiments at pressures lower than 1.2 atm or using a mixed argon/hydrogen atmosphere confirmed that the reaction rate is inversely proportional to the hydrogen concentration.

(12) Yang, G. K.; Peters, K. S.; Vaida, V. *Chem. Phys. Lett.* **1986**, *125*, 566.
(13) Photolysis of $Cr(CO)_6$ produces "naked" $Cr(CO)_5$ in perfluoromethylcyclohexane. This complex undergoes reaction ~3 orders of magnitude faster than it does in cyclohexane: Gelb, R. I.; Schwartz, L. M.; Radeos, M.; Laufer, D. A. *J. Phys. Chem.* **1983**, *87*, 3349.
(14) Wink, D. A.; Ford, P. C. *J. Am. Chem. Soc.* **1987**, *109*, 436.
(15) Halpern, J.; Wong, C. S. *J. Chem. Soc., Chem. Commun.* **1973**, 629.
(16) Gonzalez, A. A.; Zhang, K.; Nolan, S. P.; de la Vega, R. L.; Mukerjee, S. L.; Hoff, C. D.; Kubas, G. J. *Organometallics* **1988**, *7*, 2429.
(17) Darensbourg, D. J. *Adv. Organomet. Chem.* **1982**, *21*, 113.
(18) Due to the very fast nature of the reaction with pyridine, we have been able to measure directly the rate of reaction of $(P(C_6H_{11})_3)_2W(CO)_3$ only with lutidine, phosphines, and phosphites, which react at least an order of magnitude slower than pyridine. The absolute rate of reaction with pyridine is calculated from competition studies with these slower ligands, whose rates of reaction can be accurately determined on the stopped-flow apparatus: Kai, Z.; Gonzalez, A. A.; Hoff, C. D. submitted for publication in *Inorg. Chem.*
(19) Benson, S. W. *The Foundations of Chemical Kinetics*; McGraw-Hill: New York, 1960.
(20) Kubas, G. J.; Khalsa, G. R. K.; Unkefer, C. J.; Ryan, R. R. *Abstracts of Papers*, 3rd Chemical Congress of North America, Toronto, ON, Canada, June 5–10, 1988; paper 291.
(21) *IUPAC Solubility Data Series*; Battino, R., Ed.; Pergamon Press: Oxford, 1982. Data for H_2 and D_2 taken from Vol. 5/6, data for N_2 taken from Vol. 10.

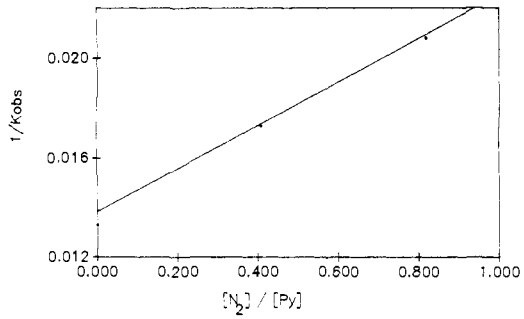

Figure 2. Plot of $1/k_{obsd}$ versus $[N_2]/[py]$ for the reaction W_5–N_2 + py → W_k–py + N_2 at 25 °C [$W_k = (P(C_6H_{11})_3)_2W(CO)_3$].

Results

Reaction of $(P(C_6H_{11})_3)_2W(CO)_3(N_2)$ with Pyridine. Replacement of coordinated nitrogen by pyridine proceeded rapidly as shown in eq 5. This reaction was studied under pseudo-

$$(P(C_6H_{11})_3)_2W(CO)_3(N_2) + py \rightarrow (P(C_6H_{11})_3)_2W(CO)_3(py) + N_2 \quad (5)$$

first-order conditions in toluene solution at a pressure of 1.2 atm N_2. Plots of ln $[A_\infty - A]$ versus time were linear through 4–5 half-lives as shown in Figure 1. Data for the rate of reaction under various conditions are shown in Table I. The mechanism of the reaction is assumed to be that shown in eq 6. This is a

$$(P(C_6H_{11})_3)_2W(CO)_3(N_2) \underset{k_{-1}}{\overset{k_1}{\rightleftharpoons}} (P(C_6H_{11})_3)_2W(CO)_3 + N_2 \quad (6)$$
$$\downarrow k_2 \text{ py}$$
$$(P(C_6H_{11})_3)_2W(CO)_3(py)$$

common type of mechanism in organometallic substitution reactions,[17] and making a steady-state assumption in $[(P(C_6H_{11})_3)_2W(CO)_3]$ leads directly to eq 7 Under pseudo-first-order

$$d[(P(C_6H_{11})_3)_2W(CO)_3(py)]/dt = k_1k_2[(P(C_6H_{11})_3)_2W(CO)_3(N_2)][py]/(k_{-1}[N_2] + k_2[py]) \quad (7)$$

conditions, a plot of $1/k_{obsd}$ versus $[N_2]/[py]$ should show a straight line with an intercept of $1/k_1$ and a slope of k_{-1}/k_1k_2.[17] A plot of this type is shown in Figure 2 where we calculate $k_{-1}/k_2 = 0.63 \pm 0.11$. We have determined independently the value of $k_2 = 8.0 \times 10^5$ M^{-1} s^{-1},[18] this allows calculation of k_{-1} as being $5.0 \pm 1.0 \times 10^5$ M^{-1} s^{-1}. From the data at 15, 25, and 35 °C, we calculate the enthalpy of activation for loss of N_2 = 17.8 ± 0.7 kcal/mol.

Reaction of $(P(C_6H_{11})_3)_2W(CO)_3(H_2)$ and -(D_2) with Pyridine. The kinetics of reaction 8 were studied under contitions similar to those described above for the dinitrogen complex. Plots of

$$(P(C_6H_{11})_3)_2W(CO)_3(H_2) + py \rightarrow (P(C_6H_{11})_3)_2W(CO)_3(py) + H_2 \quad (8)$$

A versus time did not follow simple exponential decay as observed for the dinitrogen complex described above. This is shown clearly in Figure 3, particularly where the plots of ln $[A_\infty - A]$ versus time appear to show two limiting slopes: a rapid initial formation of product followed by a slower final one. In view of the fact that the complex is known to exist in both molecular hydrogen and dihydride complexes, the mechanism shown in eq 9 was considered:

$$\begin{matrix} W_k\text{—H} \\ | \\ H \end{matrix} \underset{k_2}{\overset{k_1}{\rightleftharpoons}} W_k\text{—}(H_2) \underset{k_4}{\overset{k_3}{\rightleftharpoons}} H_2 + W_k + py \xrightarrow{k_5} W_k\text{—py} \quad (9)$$

$$W_k = (P(C_6H_{11})_3)_2W(CO)_3$$

The rate of production of product is clearly

$$d[W_k\text{–py}]/dt = k_5[W_k][py] \quad (10)$$

Assuming a steady state in the coordinatively unsaturated intermediate $W_k = (P(C_6H_{11})_3)_2W(CO)_3$ leads to

$$[W_k] = k_3[W_k\text{–}(H_2)]/(k_4[H_2] + k_5[py]) \quad (11)$$

and

$$\frac{d[W_k\text{–py}]}{dt} = \frac{k_3k_5[(P(C_6H_{11})_3)_2W(CO)_3(H_2)][py]}{k_4[H_2] + k_5[py]}$$

Under pseudo-first-order conditions where $[W_k] \ll [H_2]$ and [py], eq 9 reduces to

$$\begin{matrix} W_k\text{—H} \\ | \\ H \end{matrix} \underset{k_2}{\overset{k_1}{\rightleftharpoons}} W_k\text{—}(H_2) + py \xrightarrow{k_3'} W_k\text{—py} \quad (12)$$

where

$$k_3' = k_3k_5[py]/(k_4[H_2] + k_5[py]) \quad (13)$$

This equation can be solved by standard kinetic techniques[19] and is of the form

$$[W_k\text{–py}]_\infty - [W_k\text{–py}] = ae^{-Y_1t} + be^{-Y_2t} \quad (14)$$

where

$$Y_1 + Y_2 = k_1 + k_2 + k_3 \quad (15)$$

$$Y_1Y_2 = k_1k_3 \quad (16)$$

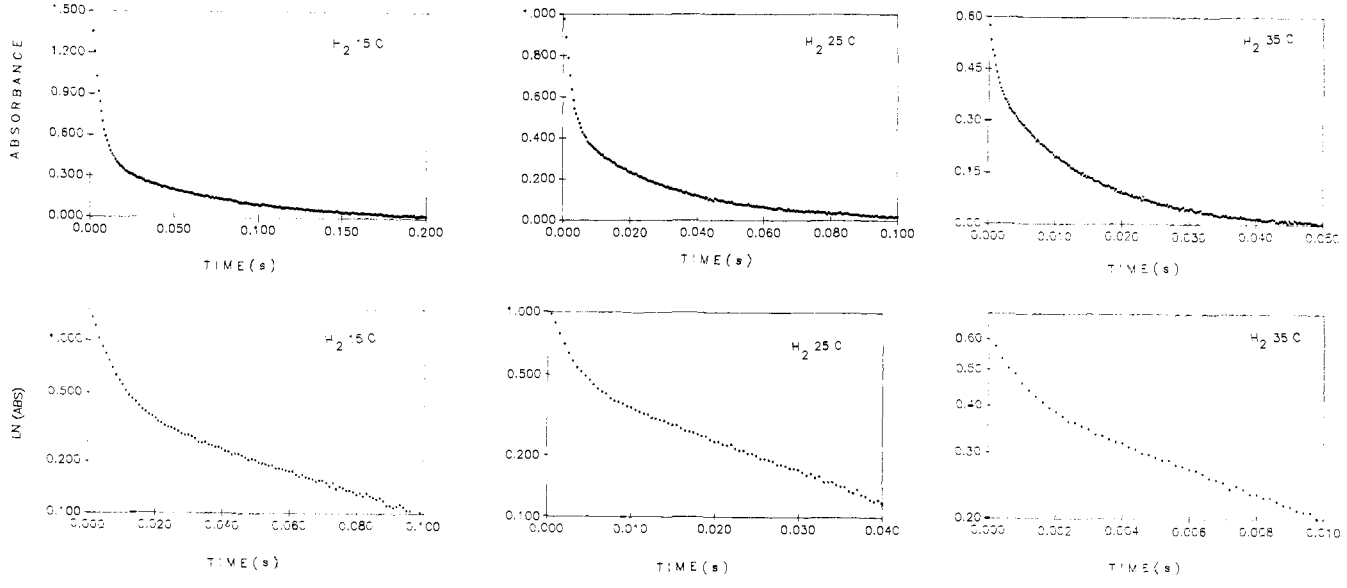

Figure 3. Plots of $A_\infty - A$ on linear (upper) and logarithmic (lower) scales for the reaction W_k–H_2 + py → W_k–py + H_2 [$W_k = (P(C_6H_{11})_3)_2W(CO)_3$] at temperatures of 15, 25, and 35 °C.

Table II. Experimental Data for the Reaction[a] $(P(C_6H_{11})_3)_2W(CO)_3H_2 + py \rightarrow (P(C_6H_{11})_3)_2W(CO)_3py + H_2$

W_k–	T, °C	$[H_2]/[py]$[b]	Y_1,[c] s^{-1}	Y_2,[c] s^{-1}	a/b[c]
H_2	35	0	1178	75	0.51
D_2	35	0	690	71	1.17
H_2	25	0	489	35.7	1.35
D_2	25	0	286	30.9	3.61
H_2	15	0	176	14.6	2.74
D_2	15	0	112	13.2	4.70
H_2	15	0.218	109	11.6	1.45
H_2	15	0.546	74	11.7	1.22

[a] Reactions performed in toluene solution under pseudo-first-order conditions as described in text. [b] Reactions performed under H_2 atmosphere; $[H_2]/[py]$ ratios calculations based on known gas solubility data.[11] Values listed as 0 were done under H_2 but at high concentration of pyridine such that $[H_2]/[py] < 0.001$. [c] Experimental data fit to the equation $\ln [A_\infty - A] = ae^{-Y_1t} + be^{-Y_2t}$ as described in the text.

Table III. Calculated Rate Constants[a] for the Reaction $(P(C_6H_{11})_3)_2W(CO)_3H_2 + py \rightarrow (P(C_6H_{11})_3)_2W(CO)_3py + H_2$

W_k–	T, °C	$[H_2]/[py]$	k_3',[b] s^{-1}	k_1, s^{-1}
H_2	35	0	1136	78
D_2	35	0	648	75
H_2	25	0	469	37
D_2	25	0	267	33
H_2	15	0	167	15.3
D_2	15	0	104	14.2
H_2	15	0.218	102	12.4
H_2	15	0.546	67	13.0

[a] Rate constants are calculated from the data in Table II, as described in the text. [b] Rate constant data calculated for k_3' can be related to k_3 by eq 13 in the text.

The values of a and b, in particular the a/b ratio, depend upon the initial conditions. If at time $t = 0$ s, the concentrations of $W_k(-H)_2$ and $W_k-(H_2)$ are in equilibrium then it can be shown that

$$\frac{Y_2 + (a/b)Y_1}{1 + a/b} = \frac{k_1k_3}{k_1 + k_2} \qquad (17)$$

It is relatively straightforward to solve for the exponentials in eq 14, and these data are collected in Table II. Each entry is the average of six to eight measurements. The agreement between calculated and experimental traces was excellent.

Conversion of the data in Table II of the exponential values to the rate constant data shown in Table III requires additional comment. In view of the fact that the two exponential roots are more than an order of magnitude apart, to a first approximation it might be expected that the two limiting exponential decay rates would correspond to k_1 and k_3, since the reaction could be viewed to occur as shown in eq 18. Examination of the data in Tables

$$W_k(-H)(-H) \xrightarrow{k_1} W_k-(H_2) + py \xrightarrow{k_3} W_k-py \qquad (18)$$

II and III shows that this is nearly the case. Calculated values for k_1 and k_3 agree within 10% with the exponential roots. In order to solve exactly for k_1, k_2, and k_3, eq 17 must be used. This equation assumes that at time $t = 0$, the molecular hydrogen and dihydride forms are at equilibrium ratios. Due to the very fast nature of this reaction, the effective half-life for decay of the molecular hydrogen complex is on the order of 0.6, 1.5, and 4 ms at 35, 25, and 15 °C. The dead time on the stopped-flow apparatus is on the order of 0.7 ms, and so only at 15 °C are the initial values near the equilibrium values (~10% of the complex reacts during the dead time). These data can then be used to solve for k_1 and k_2 at 15 °C. The ratio of k_2/k_1 at this temperature is ~0.3. This is in rough agreement with NMR studies[1,20] which also show that there is only a small change in k_2/k_1 with temperature. For purposes of calculating k_1 and k_3, these values are not very sensitive to the k_2/k_1 ratio. For the temperatures 25 and 35 °C, we assumed $k_2/k_1 = 0.5 \pm 0.3$. This assumption introduces errors

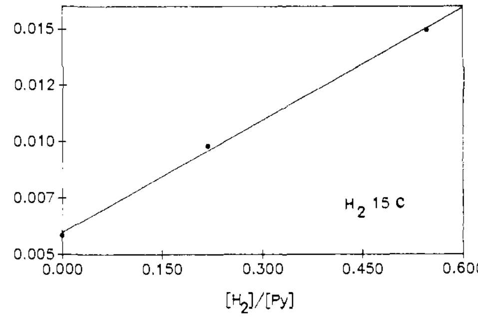

Figure 4. Plot of $1/k_{obsd}$ versus $[H_2]/[py]$ for the reaction $W_k-H_2 + py \rightarrow W_k-py + H_2$ at 15 °C ($W_k = (P(C_6H_{11})_3)_2W(CO)_3$).

in k_1 and k_3 much smaller than the estimated 10% experimental error. For the specific exponential roots shown in Table II, as a function of the k_2/k_1 ratio, k_2 appears to grow largely at the expense of the much larger k_3 with little change in k_1. The calculated rate constants in Table III are considered accurate to ±15%.

Data for k_3' shown in Table III are converted to values for k_3 through eq 13. It is clear that, for $k_5[py] \gg k_4[H_2]$, $k_3' = k_3$. At 25 and 35 °C, a large excess of pyridine was used to obtain this limiting value. Under these conditions, doubling the pyridine concentration resulted in no apparent change in the rate of reaction. At 15 °C we studied the rate of reaction as a function of $[py]/[H_2]$. From the graphical treatment shown in Figure 4, we calculate $k_4/k_5 = 2.8 \pm 0.3$. Since the rate of reaction with pyridine shows a second-order rate constant $k_5 = 8 \times 10^5$ M^{-1} s^{-1} at 25 °C,[18] the rate of reaction with molecular hydrogen is calculated to be $2.2 \pm 0.3 \times 10^6$ M^{-1} s^{-1}, based on the selectivity factor of 2.8 ± 0.3. Thus, reaction with molecular hydrogen is 4.4 ± 1.8 times *faster* than reaction with nitrogen.

The data in Table III can be used to calculate activation energies for k_1 and k_3. The values for k_1 are $\Delta H^{\ddagger} = 14.4 \pm 0.5$ and 14.7 ± 0.8 kcal/mol for H_2 and D_2, respectively. For k_3 we calculate $\Delta H^{\ddagger} = 16.9 \pm 2.2$ and 16.2 ± 1.1 kcal/mol for H_2 and D_2, respectively. Within experimental error there is no difference in activation energies for the H_2 and D_2 complexes. It should be noted that k_3 shows a significant isotope effect: $k^H/k^D = 1.7 \pm 0.1$ over the three temperatures. A much smaller effect is shown in k_1, where $k^H/k^D = 1.08 \pm 0.04$.

Discussion

The goal of this work was to understand the kinetic and thermodynamic factors controlling binding of nitrogen and hydrogen in the complex $(P(C_6H_{11})_3)_2W(CO)_3$. This complex, originally discovered by Kubas and co-workers,[1] is related to the intermediates $M(CO)_5$(alkane) (M = Cr, Mo, W) studied by flash photolysis[4-11] and described in the introduction. The formally five-coordinate complex actually forms a three-center "agostic" bond with one of the cyclohexyl groups of the phosphine ligand $W\cdots H-C_6H_{10}P$ occupying the sixth position. Thus, the vacant site can be viewed as being internally solvated via the alkyl group of the phosphine ligand.

This complex reversibly binds both hydrogen and nitrogen as shown in eqn 19 and 20. In addition, it has been shown that the

$$(P(C_6H_{11})_3)_2W(CO)_3(H_2) \rightleftharpoons H_2 + (P(C_6H_{11})_3)_2W(CO)_3 \qquad (19)$$

$$(P(C_6H_{11})_3)_2W(CO)_3(N_2) \rightleftharpoons N_2 + (P(C_6H_{11})_3)_2W(CO)_3 \qquad (20)$$

molecular hydrogen complex exists in solution in equilibrium with ~30% of a dihydride form as shown in eq 21. As described in

$$(P(C_6H_{11})_3)_2W(CO)_3(H_2) \rightleftharpoons (P(C_6H_{11})_3)_2W(CO)_3(-H)_2 \qquad (21)$$

more detail below, displacement of hydrogen by pyridine showed two limiting kinetic behaviors: rapid loss of coordinated molecular hydrogen and slower loss of hydrogen from the dihydride tautomer.

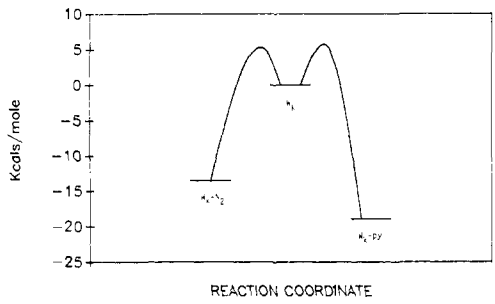

Figure 5. Reaction profile (enthalpies of reaction) for the reaction $W_k{-}N_2 \rightarrow N_2 + W_k + py \rightarrow W_k{-}py$. $W_k = (P(C_6H_{11})_3)_2W(CO)_3$ is taken as the zero point.

The more complicated kinetic behavior of the hydrogen complex was in contrast to our earlier kinetic study[16] of the pyridine complex as shown in reaction 21a. In this reaction, under

$$(P(C_6H_{11})_3)_2W(CO)_3(py) + P(OMe)_3 \rightarrow (P(C_6H_{11})_3)_2W(CO)_3(P(OMe)_3 + py \quad (21a)$$

pseudo-first-order conditions, linear plots of ln $[A_\infty - A]$ versus t were obtained through 4 or 5 half-lives. The kinetic data were consistent with the mechanism

$$W_k{-}py \underset{k_{-1}}{\overset{k_1}{\rightleftharpoons}} py + W_k + P(OMe)_3 \xrightarrow{k_3} W_k{-}P(OMe)_3 \quad (22)$$

The importance of the agostic interaction in the mechanism was shown by using the perdeuterated complex $(P(C_6D_{11})_3)_2W(CO)_3(py)$, which reacted 1.2 times more slowly than $(P(C_6H_{11})_3)_2W(CO)_3(py)$.[15] It seemed possible that failure to obtain linear plots of ln A versus time in the hydrogen complex might be due to the fact that, unlike the pyridine system, we were dealing with a gaseous ligand of relatively low solubility. For that reason, after an initial study of the H_2 complex, we investigated the N_2 complex since (i) the solubilities of nitrogen and hydrogen are similar in toluene[21] and (ii) oxidative addition of the ligand does not occur.

The kinetic behavior of the nitrogen complex was similar to that of the pyridine complex studied previously, but on a much faster time scale. The data are interpreted in terms of the mechanism shown in reaction 23. Kinetic data for this reaction

$$W_k{-}N_2 \underset{k_{-1}}{\overset{k_1}{\rightleftharpoons}} N_2 + W_k + py \xrightarrow{k_3} W_k{-}py \quad (23)$$

are collected in Table I. At high pyridine concentrations we can take $k_{obsd} = k_1$. The data in Table I can be used to calculate the activation energy for loss of N_2 as 17.8 ± 0.7 kcal/mol. These data can be combined with calorimetric data that indicate the loss of coordinated dinitrogen is endothermic by 13.5 ± 1.0 kcal/mol.[16] Therefore, the activation energy is 4.3 ± 1.7 kcal/mol higher than the ground-state energy which represents the barrier for the back-reaction as shown in the reaction profile in Figure 5. This reaction, in which N_2 replaces the W···cyclohexylphosphine agostic bond can be compared to reaction 24. There is probably little

$$Cr(CO)_5(C_6H_{12}) + CO \rightarrow Cr(CO)_6 + C_6H_{12} \quad (24)$$

kinetic difference in the reaction profile of CO with the isoelectronic N_2, and so some assessment of the role of ligands and metal can be made. The activation energy for reaction 24, 5.3 ± 1.2 kcal/mol,[9] is close to the value we obtained for the back-reaction in eq 23 of 4.3 ± 1.7 kcal/mol. The absolute values for the rates are also similar. The second-order rate constant for reaction 24 is 3.6×10^6 M^{-1} s^{-1} at 25 °C, which compares to our value of $5.0 \pm 1.0 \times 10^5$ M^{-1} s^{-1}; thus, the chromium complex $Cr(CO)_5(C_6H_{12})$ reacts only about 7 times faster than the tungsten complex $(P(C_6H_{11})_3)_2W(CO)_3$.

It is of interest to compare the rate of loss of dinitrogen ligand in this complex with other isolable dinitrogen complexes of tungsten. The rate constant of 75 s^{-1} at 25 °C corresponds to a $t_{1/2}$ of 0.009 s. Exchange of coordinated dinitrogen is fast in this complex. This can be compared to the complex $(diphos)_2W(N_2)_2$, which shows no detectable thermal dissociation of N_2 after 36 h at 70 °C.[22] It is clear that dissociation of nitrogen from these two W(O) complexes is dramatically influenced by the ligand substituents. Additional thermodynamic and kinetic studies on the binding of nitrogen are in progress.[18]

In contrast to the reaction of the nitrogen complex, reaction of the hydrogen complex did not obey simple first-order kinetics. As described in Results, the kinetic data were best interpreted in terms of the mechanism shown below the rate constants at 25 °C:

$$W_k{-}H \underset{18\ s^{-1}}{\overset{37\ s^{-1}}{\rightleftharpoons}} W_k{-}(H_2) \underset{2.2 \times 10^6\ M^{-1}\ s^{-1}}{\overset{469\ s^{-1}}{\rightleftharpoons}} H_2 + W_k + py \underset{0.125\ s^{-1}}{\overset{8 \times 10^5\ M^{-1}\ s^{-1}}{\rightleftharpoons}} W_k{-}py \quad (25)$$

Data for reaction of the hydrogen and deuterium complexes are shown in Tables II and III. Loss of coordinated D_2 is significantly slower than H_2, with $k^H/k^D = 1.7$ (0.1). A smaller kinetic isotope effect, 1.08 (0.04) is observed for conversion of the dihydride to the molecular hydrogen complex.

The kinetic isotope effect observed here is in keeping with data in the literature. It has been observed[10] that the forward reaction in eq 26 occurs 1.9 times as rapidly as the corresponding reaction

$$Cr(CO)_5(C_6H_{12}) + H_2 \rightarrow Cr(CO)_5(H_2) + C_6H_{12} \quad (26)$$

$$Cr(CO)_5(C_6H_{12}) + D_2 \rightarrow Cr(CO)_5(D_2) + C_6H_{12} \quad (27)$$

with D_2 shown in reaction 27. If it is assumed that the equilibrium constants for binding of H_2 and D_2 are similar,[23] then the reverse reaction, dissociation of H_2, should also show $k^H/k^D = 1.9$. This value is similar to our value of 1.7, and also to the value of 1.5 obtained by Wink and Ford for addition of H_2 or D_2 to $Rh(Cl)(PPh_3)_2$.[14] Since the exact nature of the transition state is not known, it is not possible to draw conclusions about the slower rate of reaction with D_2. The value $k_1^H/k_1^D = 1.08 \pm 0.04$ for the relative rates of conversion of the dihydride (dideuteride) to the molecular hydrogen (deuterium) indicates virtually no kinetic isotope effect for this reaction. The activation energies for both k_1 and k_3 overlap within experimental error for both H_2 and D_2.

The most surprising result of this study is that the rate of dissociation of molecular hydrogen is faster than the rate of oxidative addition, by at least 1 order of magnitude. While we have studied the reaction in the forward direction shown in eq 25, it is instructive to view this reaction in the reverse direction shown in eq 28. In this equation we have included approximate values

$$\begin{array}{lccccc} t_{1/2} = & & 6\ s & & 0.000032\ s & 0.04\ s \\ & W_k{-}py & \underset{+py}{\overset{-py}{\rightleftharpoons}} & W_k & \underset{-H_2}{\overset{+H_2}{\rightleftharpoons}} & W_k{-}(H_2) \rightleftharpoons W_k{-}H \\ t_{1/2} = & & 0.0014\ s & 0.0015\ s & & 0.02\ s \end{array} \quad (28)$$

for $t_{1/2}$ in seconds for each reaction at 25 °C under pseudo-firsth-order conditions ([py] = $[H_2] = 10^{-2}$ M, and $[W_k] = 5 \times 10^{-4}$ M). In the first step of reaction 28, a relatively weakly bound ligand (pyridine) dissociates to generate a vacant site at the metal on the slow time scale of seconds. The active complex W_k can react with either pyridine or hydrogen with $t_{1/2}$ values of about 140 and 32 μs, respectively. If the molecular hydrogen complex is formed, it may dissociate hydrogen and regenerate the vacant site on a time scale of ~1.5 ms or undergo oxidative addition to form the dihydride with a $t_{1/2}$ of 40 ms. Regeneration of the molecular hydrogen complex occurs with a half-life of ~20 ms. Under these conditions, the ratio of the rate of binding of molecular

(22) Carter, B. J.; Bercaw, J. E.; Gray, H. B. *J. Organomet. Chem.* **1979**, *181*, 105.

(23) Equilibrium studies appear to show that the equilibrium constants for binding of H_2 and D_2 are similar for the complex $(P(C_6H_{11})_3)_2Cr(CO)_3$; Gonzalez, A. A.; Hoff, C. D., unpublished results.

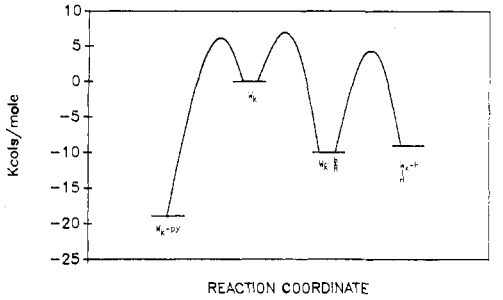

Figure 6. Reaction profile (enthalpies of reaction) for the reaction W_k–py → py + W_k + H_2 → W_k–(H_2) → W_k–($H)_2$. W_k = $(P(C_6H_{11})_3)_2W(CO)_3$ is taken as the zero point.

hydrogen to the rate of loss of coordinated molecular hydrogen to the rate of oxidative addition is roughly 1200:25:1.

Combination of the kinetic values for activation energies discussed above with thermodynamic data reported earlier allows construction of the reaction profile for eq 28 shown in Figure 6. The heats of binding of H_2 and py to $(P(C_6H_{11})_3)_2W(CO)_3$ are 10 ± 1 and 19 ± 1 kcal/mol, respectively.[16] Since the activation energy for loss of molecular hydrogen is 16.9 ± 2.2 kcal/mol, it is 6.9 ± 3.2 kcal/mol above the ground-state energy difference. This reflects the magnitude of the barrier to the back-reaction of $(P(C_6H_{11})_3)_2W(CO)_3$ with H_2. This value is somewhat higher than the value calculated for addition of nitrogen, 4.3 ± 1.7 kcal/mol. Reaction with hydrogen is ~4 times faster than with nitrogen, and this could be due to a more favorable preexponential factor for reaction with hydrogen. Since the activation energies overlap within experimental error, the apparantly higher barriers for reaction with H_2 may not be significant. Additional work regarding the entropies of these reactions is in progress.

It is clear from the above discussion that, for this system under typical conditions, molecular hydrogen will bind and dissociate many times prior to oxidative addition. This result could have importance in understanding homogeneous catalytic reactions. For example, in collaboration with others we recently studied the kinetics of the reductive elimination reactions shown in eq 29. It

$$R\text{–}Co(CO)_4 \rightleftharpoons CO + R\text{–}Co(CO)_3 \xrightarrow{H_2} R\text{–}H + H\text{–}Co(CO)_4 \qquad (29)$$

$$R = CH_2COOEt,\ C(O)(OEt)$$

was observed[24] that the net rate of reductive elimination with H_2 was some 1500 (R = $EtOOCCH_2$) to 150 (R = EtOOC) times slower than the rate of incorporation of ^{13}CO. At that time it was suggested by one of us[25] that the origin of the lowered reactivity with H_2 had to be due to electronic factors. A similar argument was made by Wink and Ford[14] to explain the lower rate of binding of H_2 compared to CO (~700 times slower) in the complex $Rh(Cl)(PPh_3)_2$. *It seems likely that this electronic effect is due to the barrier to breaking the H–H bond in the coordinated molecular hydrogen complex rather than to binding of molecular hydrogen.* To our knowledge, these are the first direct kinetic data demonstrating this for a complex in solution.

The simple reaction shown in eq 1 masks the complexity of the reaction profile with hydrogen. The complex $(P(C_6H_{11})_3)_2W(CO)_3$ strikes a balance between the several possible reactions shown in this equation. The potential energy surface for these reactions is likely to change dramatically as a function of the specific complex involved. It can be anticipated that additional reaction pathways not previously considered remain to be discovered—for example, coordination of trihydrogen in the complex $(C_5H_5)Ir(PMe_3)(H_3)^+$ has recently been reported.[26] A number of challenging problems remain in understanding the coordination chemistry of relatively simple molecules such as H_2 and N_2. Additional thermodynamic and kinetic studies are in progress on this and related group VI complexes.

Acknowledgment. Support of this work by the National Science Foundation (Grant No. CHE-8618753) is gratefully acknowledged. Special thanks are due to Mr. Daniel Taveras and Professor Nita Lewis at the University of Miami for allowing us to use the stopped-flow equipment. We also thank Dr. Gregory J. Kubas and Dr. G. R. K. Khalsa of Los Alamos National Laboratory for helpful discussions.

Registry No. $(P(C_6H_{11})_3)_2W(CO)_3(H_2)$, 104198-75-6; $(P(C_6H_{11})_3)_2W(CO)_3(D_2)$, 115380-57-9; $(P(C_6H_{11})_3)_2W(CO)_3(N_2)$, 73690-57-0; $(P(C_6H_{11})_3)_2W(CO)_3$, 73690-56-9; N_2, 7727-37-9; H_2, 1333-74-0; pyridine, 110-86-1.

(24) Hoff, C. D.; Ungváry, F.; King, R. B.; Markó, L. *J. Am. Chem. Soc.* **1985**, *107*, 666.
(25) This suggestion in ref 24 was originally made by Professor L. Markó.
(26) Heinekey, D. M.; Payne, N. G.; Schulte, G. K. *J. Am. Chem. Soc.* **1988**, *110*, 2303.